MEAN SQUARE ANALYSIS OF THE CLMS AND ACLMS FOR NON-CIRCULAR SIGNALS: THE APPROXIMATE UNCORRELATING TRANSFORM APPROACH

Danilo P. Mandic, Sithan Kanna* and Scott C. Douglas†*

*Imperial College London, Department of Electrical and Electronic Engineering, SW7 2AZ, U.K.
†Southern Methodist University, Department of Electrical Engineering, TX 75275-0338, U.S.A
Emails: {d.mandic, ssk08}@ic.ac.uk, douglas@engr.smu.edu

ABSTRACT

Current approaches to the mean-square analyses of the complex-least-mean-square (CLMS) and augmented CLMS (ACLMS) algorithms can be challenging due to the difficulty in diagonalising the augmented covariance matrix. By employing the recently introduced approximate uncorrelating transform (AUT), which diagonalizes the covariance and pseudocovariance matrices with a single singular value decomposition (SVD), we derive closed form expressions for both transient and steady-state mean square stability for the CLMS and ACLMS. Relationships between the degree of circularity of the input signal and the bound on the step-sizes of the CLMS and ACLMS are also established. We also show that for both CLMS and ACLMS, the steady-state misadjustment increases with the degree of non-circularity of the input signal. Simulations in the context of frequency estimation in power grid support the analyses.

***Index Terms*—** Complex least mean square (CLMS), augmented statistics, mean square convergence, non-circularity.

1. INTRODUCTION

The standard complex least mean square (CLMS) [1] uses a data model where at time k, the desired signal $d_k \in \mathbb{C}$, and input vector, $\mathbf{x}_k \in \mathbb{C}^{L\times 1}$, are related via the so-called strictly linear relationship given by $d_k = \mathbf{h}_{\text{opt}}^H \mathbf{x}_k + \eta_k$ where $\mathbf{h}_{\text{opt}} \in \mathbb{C}^{L\times 1}$ is an unknown optimal weight vector, $\eta_k \sim \mathcal{N}(0, \sigma_\eta^2)$ is white noise, and $(\cdot)^H$ denotes the Hermitian transpose operator.

The CLMS estimates the set of system parameters $\mathbf{h}_{\text{opt}}$, by minimising the instantaneous squared error cost function $J_k = e_k e_k^*$, where the error $e_k = d_k - \mathbf{h}_k^H \mathbf{x}_k$ and vector $\mathbf{h}_k$ is the CLMS estimate of the optimal weight vector, $\mathbf{h}_{\text{opt}}$, to give the weight update equation

$$\mathbf{h}_{k+1} = \mathbf{h}_k + \mu e_k^* \mathbf{x}_k \tag{1}$$

where the parameter μ is the step-size [2].

The standard strictly linear approach to adaptive filtering is restrictive for a general class of complex-valued signals for which the powers in the real and imaginary parts are different (second order non-circularity, improperness) [3, 4]. To this end, the widely linear approach for adaptive filtering uses an augmented input vector, $\mathbf{z}_k = [\mathbf{x}_k^T \ \mathbf{x}_k^H]^T \in \mathbb{C}^{2L\times 1}$ and augmented weight vector $\mathbf{w}_{\text{opt}} = [\mathbf{h}_{\text{opt}}^T \ \mathbf{g}_{\text{opt}}^T]^T \in \mathbb{C}^{2L\times 1}$, to give $d_k = \mathbf{w}_{\text{opt}}^H \mathbf{z}_k + \eta_k$. Estimating the augmented optimal weight vector $\mathbf{w}_{\text{opt}}$ requires the augmented CLMS (ACLMS) algorithm which is given by [5]

$$\mathbf{w}_{k+1} = \mathbf{w}_k + \mu e_k^* \mathbf{z}_k \tag{2}$$

where the output error $e_k = d_k - \mathbf{w}_k^H \mathbf{z}_k$.

The term "augmented" is used instead of widely linear for convenience, and to indicate that widely linear estimators are able to use the complete second-order (augmented) statistics of the signal by exploiting both the covariance matrix, $\mathbf{R} = \mathsf{E}\left[\mathbf{x}_k \mathbf{x}_k^H\right]$ and pseudocovariance matrix $\mathbf{P} = \mathsf{E}\left[\mathbf{x}_k \mathbf{x}_k^T\right]$ which are contained within the augmented covariance matrix

$$\mathbf{R}^a = \mathsf{E}\left[\mathbf{z}_k \mathbf{z}_k^H\right] = \mathsf{E}\begin{bmatrix}\mathbf{x}_k \\ \mathbf{x}_k^*\end{bmatrix}\begin{bmatrix}\mathbf{x}_k^H & \mathbf{x}_k^T\end{bmatrix} = \begin{bmatrix}\mathbf{R} & \mathbf{P} \\ \mathbf{P}^* & \mathbf{R}^*\end{bmatrix} \tag{3}$$

where $\mathsf{E}[\cdot]$ is the statistical expectation operator. The input vector $\mathbf{x}_k$ is said to be second-order circular (proper) if it has a vanishing pseudocovariance ($\mathbf{P} = \mathbf{0}$).

The transient and steady-state mean square analyses of the CLMS and ACLMS algorithms are challenging because they require a simultaneous diagonalization of both the covariance matrix $\mathbf{R}$ and pseudocovariance matrix $\mathbf{P}$. For the CLMS, standard approaches inherently assume that the data is circular, such as in the seminal paper by Horowitz and Senne [6]. By applying the strong uncorrelating transform (SUT) [7, 8, 9] which diagonalizes the covariance matrix $\mathbf{R}$ and pseudocovariance matrix $\mathbf{P}$ via two separate singular value decompositions (SVD), the mean square analysis for the CLMS was conducted in [10] without assuming that the input signal was circular. Using the SUT to analyse the behavior of the ACLMS algorithm requires calculating the SUT which can be difficult in practice, and it obscures any performance relationship caused by the degree of non-cirularity of the input signal.

Recently, the approximate uncorrelating transform (AUT) was introduced in order to diagonalize both the covariance and pseudocovariance matrices with a single SVD [11]. The AUT allows for both simpler analysis and a clearer physical insight into the behaviour of widely linear adaptive filters. For example, the AUT based derivation for the mean convergence behaviour of the ACLMS in [11] was easier and more intuitive to interpret compared to the SUT-based analysis in [12].

The aim of this work is to revisit the CLMS and ACLMS, and to:

1. present closed form expressions for the transient and steady-state mean square behaviour using the AUT;
2. find the relationship between the bounds for the maximum step-size against the degree of non-circularity[1] of the input;
3. establish relationships between the steady-state misadjustment and the degree of non-circularity.

The analysis is supported by illustrative simulations, including a study in the context of power grid frequency estimation.

[1] The degree of non-circularity, ρ, of a complex random variable x can be measured by the ratio of its pseudocovariance, $p = \mathsf{E}\left[x^2\right]$, to its covariance, $c = \mathsf{E}\left[|x|^2\right]$, to give $\rho = p/c$ [13].

2. DIAGONALIZING THE COVARIANCE AND PSEUDOCOVARIANCE MATRICES

Recall that for an input vector $\mathbf{x}_k$, the covariance matrix is $\mathbf{R} = \mathsf{E}\left[\mathbf{x}_k\mathbf{x}_k^H\right]$ and pseudocovariance matrix is $\mathbf{P} = \mathsf{E}\left[\mathbf{x}_k\mathbf{x}_k^T\right]$. The Takagi factorization states that any complex symmetric matrix, like the pseudocovariance matrix $\mathbf{P}^T = \mathbf{P}$, can be diagonalized as

$$\mathbf{P} = \mathbf{Q}\mathbf{\Lambda_p}\mathbf{Q}^T \tag{4}$$

where $\mathbf{Q}$ is a unitary matrix, $\mathbf{Q}\mathbf{Q}^H = \mathbf{I}$, and $\mathbf{\Lambda_p}$ is a diagonal matrix of real-valued entries, $\mathbf{\Lambda_p} = \text{diag}\{p_{\max}, \ldots, p_{\min}\}$ of circularity coefficients p_i. The approximate uncorrelating transform (AUT) states that the same matrix $\mathbf{Q}$ can be used to approximately diagonalize the covariance matrix $\mathbf{R}$, so that [11]

$$\mathbf{R} \approx \mathbf{Q}\mathbf{\Lambda_r}\mathbf{Q}^H \tag{5}$$

where $\mathbf{\Lambda_r} = \text{diag}\{\lambda_{\max}, \ldots, \lambda_{\min}\}$ and λ_i are the eigenvalues. An additional benefit of the AUT is that it allows for the diagonalisation of the pseudocovariance $\mathbf{P}$ directly while the SUT [8] requires the diagonalisation of $\mathbf{R}^{-\frac{1}{2}}\mathbf{P}\mathbf{R}^{-\frac{T}{2}}$. The approximation in (5) is valid for univariate data, and its benefits in obtaining closed form solutions for the mean square performance of the CLMS and ACLMS are shown in Sections 3 and 4.

3. MEAN SQUARE ANALYSIS OF THE CLMS

The mean square performance of the CLMS and ACLMS is analysed through the evolution of the weight error covariance [14]. The weight error vector for the CLMS is obtained by subtracting the optimal weights $\mathbf{h}_{\text{opt}}$ from both sides of equation (1), to give

$$\tilde{\mathbf{h}}_{k+1} = \tilde{\mathbf{h}}_k - \mu\mathbf{x}_k\mathbf{x}_k^H\tilde{\mathbf{h}}_k - \mu\mathbf{x}_k\eta_k^* \tag{6}$$

where $\tilde{\mathbf{h}}_k = \mathbf{h}_{\text{opt}} - \mathbf{h}_k$. To find the evolution of the weight error covariance matrix $\mathbf{K}_k \triangleq \mathsf{E}\left[\tilde{\mathbf{h}}_k\tilde{\mathbf{h}}_k^H\right]$, both sides of (6) are first multiplied by $\tilde{\mathbf{h}}_{k+1}^H$ to give

$$\begin{aligned}\tilde{\mathbf{h}}_{k+1}\tilde{\mathbf{h}}_{k+1}^H = \tilde{\mathbf{h}}_k\tilde{\mathbf{h}}_k^H &- \mu\tilde{\mathbf{h}}_k\tilde{\mathbf{h}}_k^H\mathbf{x}_k\mathbf{x}_k^H - \mu\mathbf{x}_k\mathbf{x}_k^H\tilde{\mathbf{h}}_k\tilde{\mathbf{h}}_k^H \\ &+ \mu^2\mathbf{x}_k\mathbf{x}_k^H\tilde{\mathbf{h}}_k\tilde{\mathbf{h}}_k^H\mathbf{x}_k\mathbf{x}_k^H + \mu^2\mathbf{x}_k\mathbf{x}_k^H|\eta_k|^2 \\ &+ \text{cross-terms}\end{aligned} \tag{7}$$

Upon taking the statistical expectation $\mathsf{E}[\cdot]$ of (7) and using the well-known independence assumption [15], we arrive at

$$\begin{aligned}\mathbf{K}_{k+1} = \quad &\mathbf{K}_k - \mu\mathbf{K}_k\mathbf{R} - \mu\mathbf{R}\mathbf{K}_k + \mu^2\sigma_\eta^2\mathbf{R} \\ &+\mu^2(\mathbf{R}\mathbf{K}_k\mathbf{R} + \mathbf{P}\mathbf{K}_k^T\mathbf{P}^* + \mathbf{R}\mathsf{Tr}[\mathbf{K}_k\mathbf{R}])\end{aligned} \tag{8}$$

where the Gaussian moment factorizing theorem was employed to decompose the fourth order moments in (7) as

$$\mathsf{E}\left[\mathbf{x}_k\mathbf{x}_k^H\tilde{\mathbf{h}}_k\tilde{\mathbf{h}}_k^H\mathbf{x}_k\mathbf{x}_k^H\right] = \mathbf{R}\mathbf{K}_k\mathbf{R} + \mathbf{P}\mathbf{K}_k^T\mathbf{P}^* + \mathbf{R}\mathsf{Tr}[\mathbf{K}_k\mathbf{R}]$$

Pre– and post– multiplying both sides of (8) with the unitary matrices $\mathbf{Q}^H$ and $\mathbf{Q}$, defined in (4), rotates the weight error covariance matrix to

$$\tilde{\mathbf{K}}_k \triangleq \mathbf{Q}^H\mathbf{K}_k\mathbf{Q} \tag{9}$$

The evolution of $\mathbf{K}_k$ is now given by

$$\begin{aligned}\tilde{\mathbf{K}}_{k+1} = \tilde{\mathbf{K}}_k &- \mu\tilde{\mathbf{K}}_k\mathbf{\Lambda_r} - \mu\mathbf{\Lambda_r}\tilde{\mathbf{K}}_k + \mu^2\sigma_\eta^2\mathbf{\Lambda_r} \\ &+ \mu^2(\mathbf{\Lambda_r}\tilde{\mathbf{K}}_k\mathbf{\Lambda_r} + \mathbf{\Lambda_p}\tilde{\mathbf{K}}_k^T\mathbf{\Lambda_p} + \mathbf{\Lambda_r}\mathsf{Tr}[\tilde{\mathbf{K}}_k\mathbf{\Lambda_r}])\end{aligned} \tag{10}$$

where according to the AUT, $\mathbf{\Lambda_p} = \mathbf{Q}^H\mathbf{P}\mathbf{Q}^*$ and $\mathbf{\Lambda_r} \approx \mathbf{Q}^H\mathbf{R}\mathbf{Q}$. For each diagonal term of $\tilde{\mathbf{K}}_k$, denoted by $\kappa_{ii,k}$, we have

$$\begin{aligned}\kappa_{ii,k+1} = (1-\mu\lambda_i)^2\kappa_{ii,k} &+ \mu^2(p_i^2\kappa_{ii,k} + \lambda_i\mathsf{Tr}[\tilde{\mathbf{K}}_k\mathbf{\Lambda_r}]) \\ &+ \mu^2\sigma_\eta^2\lambda_i\end{aligned} \tag{11}$$

where λ_i and p_i are respectively the diagonal terms of $\mathbf{\Lambda_r}$ and $\mathbf{\Lambda_p}$. It is convenient to collect all the diagonal terms of $\tilde{\mathbf{K}}_k$ into an $L \times 1$ vector $\boldsymbol{\kappa}_k = [\kappa_{11,k}, \ \ldots \ , \kappa_{LL,k}]^T$ to yield

$$\boldsymbol{\kappa}_{k+1} = \underbrace{\left[(\mathbf{I}-\mu\mathbf{\Lambda_r})^2 + \mu^2\mathbf{\Lambda_p}^2 + \mu^2\boldsymbol{\lambda}\boldsymbol{\lambda}^T\right]}_{\mathbf{A}}\boldsymbol{\kappa}_k + \mu^2\sigma_\eta^2\boldsymbol{\lambda} \tag{12}$$

where $\boldsymbol{\lambda} = [\lambda_{\max}, \ \ldots \ , \lambda_{\min}]^T$ is an $L \times 1$ column vector containing the eigenvalues of $\mathbf{R}$.

3.1. Mean Square Stability

For the recursion in (12) to converge, the eigenvalues of $\mathbf{A}$ have to be less than unity. Instead of attempting to determine the eigenvalues of $\mathbf{A}$ directly [16, 17], using the Gantmacher theorem [18] or using the z-domain [6], we utilize the Weyl inequality which states that for two $L \times L$ Hermitian matrices $\mathbf{X}$ and $\mathbf{Y}$

$$\bar{\lambda}\left[\mathbf{X}+\mathbf{Y}\right] \leq \bar{\lambda}\left[\mathbf{X}\right] + \bar{\lambda}\left[\mathbf{Y}\right] \tag{13}$$

where the $\bar{\lambda}\left[\cdot\right]$ operator denotes the maximum eigenvalue [19]. Applying this inequality to $\mathbf{A}$ in (12) yields

$$\bar{\lambda}\left[\mathbf{A}\right] \leq \bar{\lambda}\left[(\mathbf{I}-\mu\mathbf{\Lambda_r})^2\right] + \mu^2\left(\bar{\lambda}\left[\mathbf{\Lambda_p}^2\right] + \bar{\lambda}\left[\boldsymbol{\lambda}\boldsymbol{\lambda}^T\right]\right) \tag{14}$$

so that the condition $\bar{\lambda}\left[\mathbf{A}\right] < 1$ can be replaced with

$$1 - 2\mu\lambda_{\min} + \mu^2\left(\lambda_{\max}^2 + p_{\max}^2 + \mathsf{Tr}[\mathbf{\Lambda_r}^2]\right) < 1 \tag{15}$$

where $\lambda_{\min}$ and $\lambda_{\max}$ are the minimum and maximum eigenvalues of the covariance matrix $\mathbf{R}$ and $p_{\max}$ is the maximum singular value of the pseudo-covariance matrix $\mathbf{P}$. The inequality in (15) still holds if $\mathsf{Tr}[\mathbf{\Lambda_r}^2]$ is replaced by $L\lambda_{\max}^2$ and therefore the CLMS achieves mean square stability for

$$0 < \mu < \frac{2}{s[\mathbf{R}]\lambda_{\max}(1+L+|\rho|^2)} \tag{16}$$

where $\lambda_{\max}$ and $s[\mathbf{R}] = \lambda_{\max}/\lambda_{\min}$ are respectively the maximum eigenvalue and eigenvalue spread of the covariance matrix $\mathbf{R}$. The term $|\rho|^2 = p_{\max}^2/\lambda_{\max}^2$ can be interpreted as the maximum circularity coefficient of the input.

Remark #1: The maximum step-size for mean square stability is inversely proportional to the degree of circularity, $|\rho|$.

3.2. Steady State Analysis

The steady-state value of $\boldsymbol{\kappa}_k$ in (12) is given by

$$\boldsymbol{\kappa}_\infty = \left[2\mathbf{\Lambda_r} - \mu(\mathbf{\Lambda_p}^2 + \mathbf{\Lambda_r}^2) - \mu\boldsymbol{\lambda}\boldsymbol{\lambda}^T\right]^{-1}\mu\sigma_\eta^2\boldsymbol{\lambda} \tag{17}$$

Upon employing the matrix inversion lemma, the steady state misadjustment can be expressed as

$$M_{\text{CLMS}} = \frac{\boldsymbol{\lambda}^T\boldsymbol{\kappa}_\infty}{\sigma_\eta^2} = \frac{\displaystyle\sum_{j=1}^{L}\frac{\mu\lambda_j}{2-\mu\lambda_j(1+|\rho_j|^2)}}{1-\displaystyle\sum_{j=1}^{L}\frac{\mu\lambda_j}{2-\mu\lambda_j(1+|\rho_j|^2)}} \tag{18}$$

Remark #2: The steady-state misadjustment of the CLMS algorithm increases with the increase in the non-circularity of the input signal. This is easily verified through the first derivative of the misadjustment M_{CLMS} with respect to the circularity coefficient $|\rho|$, which gives $(\partial M_{\text{CLMS}}/\partial|\rho|) > 0$.

4. MEAN SQUARE ANALYSIS OF THE ACLMS

A similar analysis is carried out for the ACLMS whereby the input and weight vectors within the CLMS are replaced by the augmented vectors that are twice the length of the vectors in the CLMS equations. The widely linear data model is given by $d_k = \mathbf{h}_{\text{opt}}^H \mathbf{x}_k + \mathbf{g}_{\text{opt}}^H \mathbf{x}_k^* + \eta_k$, so that the augmented weight error vector recursion from (2) becomes

$$\tilde{\mathbf{w}}_{k+1} = \tilde{\mathbf{w}}_k - \mu \mathbf{z}_k \mathbf{z}_k^H \tilde{\mathbf{w}}_k - \mu \mathbf{z}_k \eta_k^* \tag{19}$$

where $\tilde{\mathbf{w}}_k = \left[\mathbf{h}_{\text{opt}}^T - \mathbf{h}_k^T,\ \mathbf{g}_{\text{opt}}^T - \mathbf{g}_k^T\right]^T$ while the augmented weight error covariance matrix is $\mathbf{K}_k^a = \mathsf{E}\left[\tilde{\mathbf{w}}_k \tilde{\mathbf{w}}_k^H\right]$. By multiplying both sides of (19) by $\tilde{\mathbf{w}}_{k+1}^H$, we have

$$\begin{aligned}\tilde{\mathbf{w}}_{k+1}\tilde{\mathbf{w}}_{k+1}^H = \tilde{\mathbf{w}}_k\tilde{\mathbf{w}}_k^H - \mu\tilde{\mathbf{w}}_k\tilde{\mathbf{w}}_k^H\mathbf{z}_k\mathbf{z}_k^H - \mu\mathbf{z}_k\mathbf{z}_k^H\tilde{\mathbf{w}}_k\tilde{\mathbf{w}}_k^H \\ + \mu^2\mathbf{z}_k\mathbf{z}_k^H\tilde{\mathbf{w}}_k\tilde{\mathbf{w}}_k^H\mathbf{z}_k\mathbf{z}_k^H + \mu^2\mathbf{z}_k\mathbf{z}_k^H|\eta_k|^2 \\ + \text{cross-terms}\end{aligned} \tag{20}$$

Similarly to (8) the augmented weight error covariance matrix is

$$\begin{aligned}\mathbf{K}_{k+1}^a = \mathbf{K}_k^a - \mu\mathbf{K}_k^a\mathbf{R}^a - \mu\mathbf{R}^a\mathbf{K}_k^a + \mu^2\sigma_\eta^2\mathbf{R}^a + \\ \mu^2(\mathbf{R}^a\mathbf{K}_k^a\mathbf{R}^a + \mathbf{P}^a\mathbf{K}_k^{aT}\mathbf{P}^{a*} + \mathbf{R}^a\mathsf{Tr}[\mathbf{K}_k^a\mathbf{R}^a])\end{aligned} \tag{21}$$

where the augmented covariance matrix $\mathbf{R}^a$ is given in (3) and the augmented pseudocovariance matrix $\mathbf{P}^a$ is

$$\mathbf{P}^a = \mathsf{E}\left[\mathbf{z}_k\mathbf{z}_k^T\right] = \mathsf{E}\begin{bmatrix}\mathbf{x}_k \\ \mathbf{x}_k^*\end{bmatrix}\begin{bmatrix}\mathbf{x}_k^T & \mathbf{x}_k^H\end{bmatrix} = \begin{bmatrix}\mathbf{P} & \mathbf{R} \\ \mathbf{R}^* & \mathbf{P}^*\end{bmatrix} \tag{22}$$

Recall that the augmented covariance and pseudocovariance matrices are jointly diagonalized with the AUT as

$$\mathbf{R}^a \approx \bar{\mathbf{Q}}\mathbf{D}_{\mathbf{r}}\bar{\mathbf{Q}}^H \qquad \mathbf{P}^a = \bar{\mathbf{Q}}\mathbf{D}_{\mathbf{p}}\bar{\mathbf{Q}}^T \tag{23}$$

where the unitary matrix $\bar{\mathbf{Q}}$ consists of the unitary matrices from (4), and has the form

$$\bar{\mathbf{Q}} = \frac{1}{\sqrt{2}}\begin{bmatrix}\mathbf{Q} & -\mathbf{Q} \\ \mathbf{Q}^* & \mathbf{Q}^*\end{bmatrix}$$

The diagonal matrices $\mathbf{D}_{\mathbf{r}}$ and $\mathbf{D}_{\mathbf{p}}$ are identical except for opposite signs of the last L diagonal elements, that is

$$\begin{aligned}\mathbf{D}_{\mathbf{r}} = \begin{bmatrix}\mathbf{\Lambda}_{\mathbf{r}} + \mathbf{\Lambda}_{\mathbf{p}} & \mathbf{0} \\ \mathbf{0} & \mathbf{\Lambda}_{\mathbf{r}} - \mathbf{\Lambda}_{\mathbf{p}}\end{bmatrix} \\ \mathbf{D}_{\mathbf{p}} = \begin{bmatrix}\mathbf{\Lambda}_{\mathbf{r}} + \mathbf{\Lambda}_{\mathbf{p}} & \mathbf{0} \\ \mathbf{0} & -(\mathbf{\Lambda}_{\mathbf{r}} - \mathbf{\Lambda}_{\mathbf{p}})\end{bmatrix}\end{aligned} \tag{24}$$

The recursion in (21) can be also rotated by pre– and post– multiplying it by $\bar{\mathbf{Q}}^H$ and $\bar{\mathbf{Q}}$, so that

$$\begin{aligned}\tilde{\mathbf{K}}_{k+1}^a = \tilde{\mathbf{K}}_k^a - \mu\tilde{\mathbf{K}}_k^a\mathbf{D}_{\mathbf{r}} - \mu\mathbf{D}_{\mathbf{r}}\tilde{\mathbf{K}}_k^a + \mu^2\sigma_\eta^2\mathbf{D}_{\mathbf{r}} + \\ \mu^2(\mathbf{D}_{\mathbf{r}}\tilde{\mathbf{K}}_k^a\mathbf{D}_{\mathbf{r}} + \mathbf{D}_{\mathbf{p}}\tilde{\mathbf{K}}_k^{aT}\mathbf{D}_{\mathbf{p}} + \mathbf{D}_{\mathbf{r}}\mathsf{Tr}[\tilde{\mathbf{K}}_k^a\mathbf{D}_{\mathbf{r}}])\end{aligned} \tag{25}$$

where $\tilde{\mathbf{K}}_{k+1}^a = \bar{\mathbf{Q}}^H\mathbf{K}_k^a\bar{\mathbf{Q}}$. The diagonal elements of $\tilde{\mathbf{K}}_k^a$, denoted by $\kappa_{ii,k}^a$, then evolve according to

$$\begin{aligned}\kappa_{ii,k+1}^a = (1-\mu r_i)^2\kappa_{ii,k}^a + \mu^2(r_i^2\kappa_{ii,k}^a + r_i\mathsf{Tr}[\tilde{\mathbf{K}}_k^a\mathbf{D}_{\mathbf{r}}]) \\ + \mu^2\sigma_\eta^2 r_i\end{aligned} \tag{26}$$

where $r_i, i = 1, \ldots 2L$ are the diagonal elements of $\mathbf{D}_{\mathbf{r}}$ and $\mathbf{D}_{\mathbf{r}}^2 = \mathbf{D}_{\mathbf{p}}^2$. The diagonal elements of $\tilde{\mathbf{K}}_k^a$ are next combined into a vector $\boldsymbol{\kappa}_k^a = [\kappa_{11,k}^a,\ \ \ldots\ \ , \kappa_{2L\,2L,k}^a]^T$ and admit a vector recursion

$$\boldsymbol{\kappa}_{k+1}^a = \underbrace{\left[(\mathbf{I} - \mu\mathbf{D}_{\mathbf{r}})^2 + \mu^2\mathbf{D}_{\mathbf{r}}^2 + \mu^2\mathbf{r}\mathbf{r}^T\right]}_{\mathbf{B}}\boldsymbol{\kappa}_k^a + \mu^2\sigma_\eta^2\mathbf{r} \tag{27}$$

where $\mathbf{r} = [r_{\max},\ \ \ldots\ \ , r_{\min}]^T$ is a $2L \times 1$ vector containing the diagonal elements of $\mathbf{D}_{\mathbf{r}}$.

4.1. Mean Square Stability

The ACLMS is stable in the mean square sense if the condition $\bar{\lambda}[\mathbf{B}] < 1$ is satisfied. Applying the Weyl inequality in (13) to $\mathbf{B}$ yields

$$\bar{\lambda}[\mathbf{B}] \leq \bar{\lambda}[(\mathbf{I} - \mu\mathbf{D}_{\mathbf{r}})^2] + \mu^2\left(\bar{\lambda}[\mathbf{D}_{\mathbf{r}}^2] + \bar{\lambda}[\mathbf{r}\mathbf{r}^T]\right) \tag{28}$$

which gives to the bound on the step-size,

$$0 < \mu < \frac{2r_{\min}}{2r_{\max}^2 + 2Lr_{\max}^2} \tag{29}$$

Dividing the numerator and denominator with $r_{\min}$ and recognizing that the maximum eigenvalue of the augmented covariance matrix, $r_{\max}$, is the sum of the maximum eigenvalues of the covariance matrix, $\mathbf{R}$, and pseudocovariance matrix, $\mathbf{P}$ that is, $r_{\max} = \lambda_{\max} + p_{\max}$, gives

$$0 < \mu < \frac{1}{s[\mathbf{R}^a](\lambda_{\max} + p_{\max})(L+1)} \tag{30}$$

where the eigenvalue spread of the augmented covariance matrix is

$$s[\mathbf{R}^a] = \frac{r_{\max}}{r_{\min}} = \frac{\lambda_{\max} + p_{\max}}{\lambda_{\min} - p_{\min}}. \tag{31}$$

Remark #3: By comparing (16) and (30), notice that for circular data, since the filter order of the ACLMS is twice that of the CLMS the maximum learning rate of the ACLMS can be at most half the maximum learning rate of the CLMS.

4.2. Steady State Analysis

In steady-state, the ACLMS weight error covariance in (27) settles to

$$\boldsymbol{\kappa}_\infty^a = \left[2\mathbf{D}_{\mathbf{r}} - 2\mu\mathbf{D}_{\mathbf{r}}^2 - \mu\mathbf{r}\mathbf{r}^T\right]^{-1}\mu\sigma_\eta^2\mathbf{r} \tag{32}$$

Similarly to (18), the ACLMS misadjustment is

$$M_{\text{ACLMS}} = \frac{\mathbf{r}^T\boldsymbol{\kappa}_\infty^a}{\sigma_\eta^2} = \frac{\displaystyle\sum_{j=1}^{2L}\frac{\mu r_j}{2 - 2\mu r_j}}{1 - \displaystyle\sum_{j=1}^{2L}\frac{\mu r_j}{2 - 2\mu r_j}} \tag{33}$$

where the eigenvalues of the augmented covariance matrix are given by

$$r_j = \begin{cases}\lambda_j + p_j, & j = 1, \ldots, L \\ \lambda_j - p_j, & j = L+1, \ldots, 2L\end{cases} \tag{34}$$

Remark #4: The ACLMS has a larger misadjustment compared to the CLMS due to the additional gradient noise introduced by doubling the number of weight vectors[2]. Like the CLMS, the ACLMS has increasing misadjustment for increasingly non-circular signals.

[2]This effect can be mitigated by setting $\mu_{\text{ACLMS}} = \frac{1}{2}\mu_{\text{CLMS}}$.

5. SIMULATIONS

In the first set of simulations, the steady-state misadjustment of the CLMS and ACLMS was investigated in a system identification setting, for a strictly linear FIR channel of length $L = 2$, with coefficients $\mathbf{h}_{\text{opt}} = [0.4,\ 0.7j]^T$. The input $\mathbf{x}_k$ was a zero-mean Gaussian process with covariance matrix $\mathbf{R}$ and pseudocovariance matrix $\mathbf{P}$, given by

$$\mathbf{R} = \begin{bmatrix} r_{xx} & \alpha r_{xx} \\ \alpha^* r_{xx} & r_{xx} \end{bmatrix} \qquad \mathbf{P} = \begin{bmatrix} p_{xx} & \alpha p_{xx} \\ \alpha p_{xx} & p_{xx} \end{bmatrix} \tag{35}$$

where $r_{xx} = \dfrac{1}{1-|\alpha|^2}$, $p_{xx} = \dfrac{\rho}{1-\alpha^2}$ and $\alpha = 0.2j$. The output of the system was contaminated with circular white Gaussian noise with variance $\sigma_\eta^2 = 0.05$. For a fair comparison, the step-size of CLMS was set to $\mu_{\text{CLMS}} = 0.2$ while the ACLMS step-size was $\mu_{\text{ACLMS}} = \frac{1}{2}\mu_{\text{CLMS}} = 0.1$, see also footnote 2 [20] and [21].

The steady-state misadjustment was computed via a Monte-Carlo simulation over 50,000 independent trials and for varying degrees of input circularity ρ. Figure 1(a) shows the steady-state misadjustment of CLMS for non-circular signals, which conforms with the analysis in (18) and Remark #2.

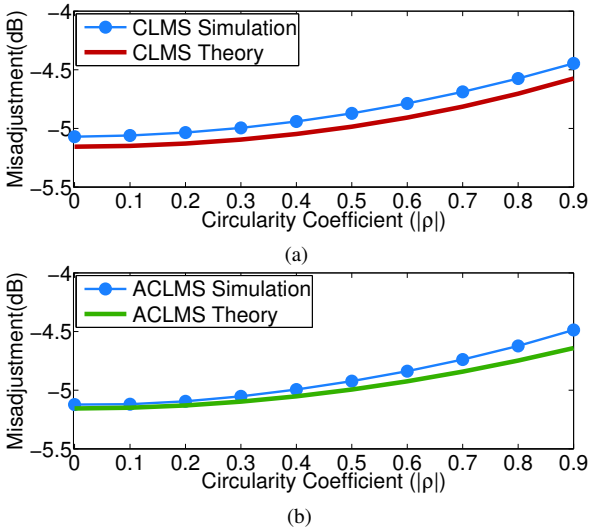

Fig. 1: Steady-state misadjustment of the (a) CLMS and (b) ACLMS algorithms for varying degrees of input circularity.

Figure 1(b) shows the misadjustment of ACLMS for varying degrees of circularity, observe a similar behaviour to the CLMS. Although the covariance matrices $\mathbf{R}$ and $\mathbf{P}$ in (35) cannot be jointly diagonalized with a single SVD, the use of AUT allowed us to estimate the theoretical misadjustment of the CLMS and ACLMS and their relationships to the circularity of the input in an intuitive, compact and physically meaningful way.

5.1. Three-phase frequency estimation

The misadjustment was next investigated for the ACLMS based three-phase frequency estimator, which estimates the frequency of a complex-valued 3-phase signal – for more information we refer to [22]. The complex-valued α-β voltage is given by

$$v_k = v_{\alpha,k} + v_{\beta,k} + \eta_k \qquad \eta_k \sim \mathcal{N}(0, \sigma_\eta^2) \tag{36}$$

and was generated by applying the Clarke's transformation to a three-phase voltage signal with angular frequency $\omega = 2\pi f_o$ and frequency, $f_o = 50$ Hz

$$\begin{bmatrix} v_{\alpha,k} \\ v_{\beta,k} \end{bmatrix} = \sqrt{\frac{2}{3}} \begin{bmatrix} 1 & -\frac{1}{2} & -\frac{1}{2} \\ 0 & \frac{\sqrt{3}}{2} & -\frac{\sqrt{3}}{2} \end{bmatrix} \text{Re}\left\{ \begin{bmatrix} \bar{V}_a \\ \bar{V}_b \\ \bar{V}_c \end{bmatrix} e^{j\omega k \Delta T} \right\} \tag{37}$$

where $\bar{V}_a$, $\bar{V}_b$ and $\bar{V}_c$ are phasor representations of the three-phase voltage and $\text{Re}\{\cdot\}$ extracts the real part of a complex variable. The sampling frequency $f_{\text{samp}} = 1/\Delta T$ was chosen to be 2 kHz. Under a general operating condition, $\bar{V}_a = \gamma$, $\bar{V}_b = -\frac{\gamma}{2} - j\frac{\sqrt{3}}{2}$ and $\bar{V}_c = -\frac{\gamma}{2} + j\frac{\sqrt{3}}{2}$. In the simulations, we used $\gamma = 1$ for a balanced system and $\gamma = 0.2$ for the Type D imbalance, see also Figure 2.

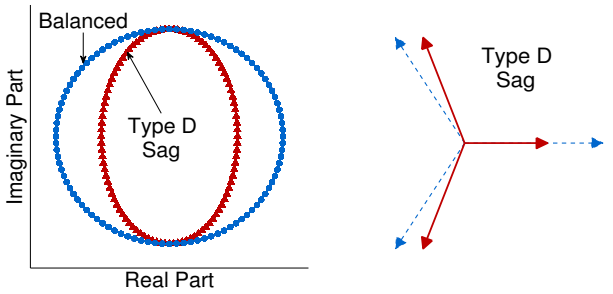

(a) Circularity plot (b) Phasor representation

Fig. 2: Geometric and phasor diagrams for a Type D imbalance (voltage sag) of the three-phase power system voltages.

Table 1 shows that the ACLMS frequency estimator has a higher misadjustment for a noncircular signal, arising from an unbalanced set of system voltages within a three-phase power system. This conforms with the analysis and Remark #4.

Data Statistics	**Misadjustment (dB)**
Balanced (*circular*)	2.2325
Type D Imbalance (*non-circular*)	2.6142

Table 1: Steady-state misadjustment values for the ACLMS-based frequency estimator. The three-phase voltage signals were generated at SNR = 30 dB.

6. CONCLUSION

We have conducted mean square stability and steady-state analyses of the CLMS and ACLMS for non-circular data. This has been achieved using the recently introduced approximate uncorrelating transform (AUT), which first diagonalises the pseudocovariance matrix and then uses the same SVD to diagonalise the covariance matrix. This has greatly simplified the analysis and has provided compact and physically meaningful relationships between the circularity of the input and the mean square behaviour of the CLMS and ACLMS. We have found that the step-size bounds of the CLMS and ACLMS are inversely proportional to the degree of circularity of the input and the steady-state misadjustment increases as the non-circularity of the input signal is increased. Simulations on benchmark and 3-phase power signals support the analysis.

7. REFERENCES

[1] B. Widrow, J. McCool, and M. Ball, "The complex LMS algorithm," *Proc. of the IEEE*, vol. 63, no. 4, pp. 719–720, 1975.

[2] D.P. Mandic and V.S.L. Goh, *Complex valued nonlinear adaptive filters: Noncircularity, widely linear and neural models*, Wiley, 2009.

[3] B. Picinbono and P. Chevalier, "Widely linear estimation with complex data," *IEEE Trans. on Signal Process.*, vol. 43, no. 8, pp. 2030–2033, 1995.

[4] P.J. Schreier, L.L. Scharf, and C.T. Mullis, "Detection and estimation of improper complex random signals," *IEEE Trans. on Inform. Theory*, vol. 51, no. 1, pp. 306–312, Jan 2005.

[5] S. Javidi, M. Pedzisz, S.L. Goh, and D.P. Mandic, "The augmented complex least mean square algorithm with application to adaptive prediction problems," in *Proc. of the 1st IARP Workshop on Cognitive Inform. Process.*, 2008, pp. 54–57.

[6] L.L. Horowitz and K.D. Senne, "Performance advantage of complex LMS for controlling narrow-band adaptive arrays," *IEEE Trans. on Acoust., Speech and Signal Process.*, vol. 29, no. 3, pp. 722–736, 1981.

[7] L. De Lathauwer and B. De Moor, "On the blind separation of non-circular sources," in *Proc. of the 11th European Signal Process. Conf. (EUSIPCO)*, 2002, pp. 99–102.

[8] J. Eriksson and V. Koivunen, "Complex random vectors and ICA models: identifiability, uniqueness, and separability," *IEEE Trans. on Inform. Theory*, vol. 52, no. 3, pp. 1017–1029, 2006.

[9] S.C. Douglas, "Fixed-point algorithms for the blind separation of arbitrary complex-valued non-Gaussian signal mixtures," *EURASIP Journal on Advances in Signal Process.*, vol. 2007, no. 1, pp. 036525, 2007.

[10] S.C. Douglas and D.P. Mandic, "Mean and mean-square analysis of the complex LMS algorithm for non-circular Gaussian signals," in *Proc. of the 13th IEEE Digital Signal Process. Workshop and 5th IEEE Signal Process. Educ. Workshop (DSP/SPE 2009)*, 2009, pp. 101–106.

[11] C. Cheong Took, S.C. Douglas, and D.P. Mandic, "On approximate diagonalization of correlation matrices in widely linear signal processing," *IEEE Trans. Signal Process.*, vol. 60, no. 3, pp. 1469–1473, 2012.

[12] S.C. Douglas and D.P. Mandic, "Performance analysis of the conventional complex LMS and augmented complex LMS algorithms," in *Proc. of the IEEE Intl. Conf. on Acoust., Speech and Signal Process. (ICASSP)*, 2010, pp. 3794–3797.

[13] E. Ollila, "On the circularity of a complex random variable," *IEEE Signal Process. Letters*, vol. 15, pp. 841–844, 2008.

[14] D.P. Mandic, Y. Xia, and S.C. Douglas, "Steady state analysis of the CLMS and augmented CLMS algorithms for noncircular complex signals," in *Proc. of the 44th Asilomar Conf. on Signals, Systems and Computers (ASILOMAR)*, 2010, pp. 1635–1639.

[15] J.E. Mazo, "On the independence theory of euqlizer convergence," *Bell Systems Technical Journal*, vol. 58, no. 5, pp. 963–966, May-June 1979.

[16] A. Feuer and E. Weinstein, "Convergence analysis of LMS filters with uncorrelated Gaussian data," *IEEE Trans. on Acoust., Speech and Signal Process.*, vol. 33, no. 1, pp. 222–230, 1985.

[17] M. Rupp and F. Hausberg, "LMS algorithmic variants in active noise and vibration control," in *Proc. of the 22nd European Signal Process. Conf. (EUSIPCO)*, Sept 2014, pp. 691–695.

[18] J.B. Foley and F.M. Boland, "A note on the convergence analysis of LMS adaptive filters with Gaussian data," *IEEE Trans. on Acoust., Speech and Signal Process.*, vol. 36, no. 7, pp. 1087–1089, 1988.

[19] A. Knutson and T. Tao, "Honeycombs and sums of Hermitian matrices," *Notices of the AMS*, vol. 48, no. 2, pp. 175–186, 2001.

[20] B. Jelfs, D. P. Mandic, and S. C. Douglas, "An adaptive approach for the identification of improper complex signals," *Signal Process.*, vol. 92, no. 2, pp. 335 – 344, 2012.

[21] D.P. Mandic, S. Still, and S.C. Douglas, "Duality between widely linear and dual channel adaptive filtering," in *Proc. of the IEEE Intl. Conf. on Acoust., Speech and Signal Process. (ICASSP)*, April 2009, pp. 1729–1732.

[22] Y. Xia, S.C. Douglas, and D.P. Mandic, "Adaptive frequency estimation in smart grid applications: Exploiting noncircularity and widely linear adaptive estimators," *IEEE Signal Process. Mag.*, vol. 29, no. 5, pp. 44–54, 2012.